PCCP

VBDFT(s)—a semi-empirical valence bond method: Application to linear polyenes containing oxygen and nitrogen heteroatoms

Wei Wu,*[a] Yan Luo,[a] Lingchun Song[a] and Sason Shaik*[b]

[a] *Department of Chemistry, The State Key Laboratory for Physical Chemistry of Solid Surfaces, and Institute of Physical Chemistry, Xiamen University, Xiamen, Fujian 361005, China. E-mail: weiwu@xmu.edu.cn*

[b] *Department of Organic Chemistry and the Lise Meitner–Minerva Center for Computational Quantum Chemistry, The Hebrew University, Jerusalem 91904, Israel. E-mail: sason@yfaat.ch.huji.ac.il*

Received 20th August 2001, Accepted 8th October 2001
First published as an Advance Article on the web

A semi-empirical valence bond (VB) method, VBDFT(s), is applied to the series of linear polyenes with heteroatoms $C_{M-1}H_MO$, $C_{M-2}H_{M-2}O_2$, $C_{M-1}H_{M+1}N$, and $C_{M-2}H_MN_2$ ($M = 4$–26). The computational results show that the VBDFT(s) method, which was first applied to linear polyenes, is also suitable for treatment of linear polyenes with polar bonds. Properties such as the wavefunction, extent of delocalization, the resonance energy, and the energy additivity are discussed.

1 Introduction

Valence bond (VB) theory[1,2] has remained one of the most powerful approaches to conceptualize and predict chemical behavior. However, the use of VB theory has always been hampered by the lack of computational methods which can treat reasonably large molecules, and which are at the same time simple enough to enable one to build up the type of insight that has been so successful in molecular orbital theory.[3]

Recently we introduced such a method called VBDFT(s).[4] This is a semi-empirical method which is scaled with a single parameter to give the energies of density functional theory (DFT), hence the name VBDFT(s). An important feature of the method is its reliance on Rumer structures[5] which are the canonical chemical structures. This feature provides a powerful facility to analyze chemical problems in terms of VB mixing diagrams based on the familiar chemical structures. The accuracy and lucidity of the method was recently demonstrated by analyzing the ground and several excited states[6] of linear polyenes. The method was shown to reproduce excitation energies close to the values obtained by sophisticated methods like CASPT2,[7,8] and in addition, it provided the means to understand trends and to project them to infinitely long systems.

An essential element of the method is the use of a set of only those structures that are formally covalent. Ionic structures are not included explicitly, and their effect is incorporated in the parameter λ.[9–12] While such an approach proved successful for polyenes where ionicity is very small, one wonders whether the method would still be applicable to systems containing heteroatoms. To this end we present here an extension of VBDFT(s) to polyene systems containing heteroatoms, O and N, as shown in Scheme 1. Here we find the appropriate single parameter that scales the VB energy to that of DFT, and in particular to the hybrid functional B3LYP. We show that despite the significant ionicity of the C=O and C=N bonds, the total energy can be scaled nicely to DFT, all the way up to systems with a significant length of 26 heavy atoms. Some trends of the ground states are discussed and compared to the all carbon systems.

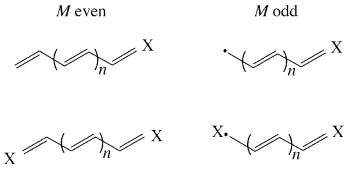

Scheme 1 Linear polyenes with heteroatoms.

2 Methodology

A brief summary of VBDFT(s)

VBDFT(s) was described elsewhere[4,6] and will be sketched only briefly in this paper. It is a Hückel-type semi-empirical VB method scaled to density functional energies by utilizing the DFT energy of the spin-alternant determinant and a parameter λ, which is the interaction term that couples one electron pair into a bond. In this sense the method has great affinity to similar work of other groups.[13–18] The zero differential overlap approximation is used in VBDFT(s), and the resulting Hamiltonian matrix has the appearance of a Hückel matrix. The Hückel parameter α is given here by the DFT energy of the spin-alternant determinant, while the parameter λ is equivalent to the Hückel resonance integral β. For ethylene, λ is a positive quantity standing for the energy difference between the π-bonded molecule and its spin-alternant determinant that possesses two unpaired p_π electrons in an antiferromagnetic arrangement (see drawing 1). Thus, as already mentioned, the parameter λ incorporates the effect of ionic structures, and the method does not require explicit consideration of these struc-

tures. Once λ is determined, the subsequent calculations rely on the canonical structures, as explained below.

Drawing 1

Spin-free form of VBDFT(s) using canonical structures

In a traditional VB approach, VB functions are expressed in terms of a linear combination of VB determinants, *i.e.*, a VB function includes 2^m VB determinants, where m is the number of covalent bonds in the structure. Obviously, the number of the VB determinants increases rapidly with the number of covalent bonds. For example, for a system of 20 electrons with 10 covalent bonds, the number of VB determinants required for a single VB function is 1024, and the VB representation of the Hamiltonian contains one million matrix elements of VB determinants. In spin-free quantum chemistry, the spin-free wavefunction, a purely spatial function of appropriate permutation symmetry, is written as

$$\Psi = \sum_i C_i \Phi_i \tag{1}$$

where the VB function Φ_i is easily described through the projector of the symmetric group S_M as follows:[19,20]

$$\Phi_i = N_i e_{r1}^{[\mu]} \Omega_i \tag{2}$$

where N_i is a normalization factor, $e_{rs}^{[\mu]}$ is the standard projector of symmetric group S_N, and Ω_i is an orbital product that corresponds to a VB structure. The Hamiltonian and overlap matrix elements are written as

$$H_{ij} = \langle \Phi_i | H | \Phi_j \rangle = \sum_{P \in S_N} D_{11}^{[\mu]}(P) \langle \Omega_i | HP | \Omega_j \rangle \tag{3}$$

and

$$M_{ij} = \langle \Phi_i \mid \Phi_j \rangle = \sum_{P \in S_N} D_{11}^{[\mu]}(P) \langle \Omega_i | P | \Omega_j \rangle, \tag{4}$$

respectively, where $D_{11}^{[\mu]}(P)$ is the irreducible representation matrix element. In the zero differential overlap approximation of the Hückel-type VBDFT(s) method, all integrals are neglected with the exception of one-electron integrals between two neighboring atoms. Eqns. (3) and (4) are greatly simplified to the forms

$$H_{ij} = E_{\rm sa} S_{ij} - \sum_{k=1}^{N-1} D_{11}^{[\mu]}(P_i^{-1}(k, k+1) P_j) \lambda_{k,k+1}, \tag{5}$$

$$M_{ij} = D_{11}^{[\mu]}(P_i^{-1}(k, k+1) P_j), \tag{6}$$

where $E_{\rm sa}$ is the energy of the spin-alternant determinant obtained by DFT,[6] and P_i is the permutation acting on electronic indexes of the fundamental Rumer structure to yield those corresponding to Rumer structure i. The value of $D_{11}^{[\mu]}(P)$ has been shown[20] to have the form $(-1)^t(-1/2)^u$, where t and u depend on the permutation and the irreducible representation $[\mu]$ and are easily determined.

With eqns. (4) and (5), the coefficients C_i in eqn. (1) are easily obtained by solving the usual secular equation $\mathbf{HC} = E\mathbf{SC}$. The weight of a VB structure can be defined as

$$W_i = \sum_j C_i S_{ij} C_j \,. \tag{7}$$

From eqn. (5), one can get an energy expression for the energy of a canonical Rumer structure by simply inspecting the structure. Thus, relative to the energy of the spin alternant determinant, the energy reads as follows:

$$E(R_i) = E_{\rm sa} - \sum_{i_b} \lambda(r_{ib}) + \frac{1}{2} \sum_{i_{nb}} \lambda(r_{i_{nb}}). \tag{8}$$

Here the first summation runs over all short bonds while the second summation is over the close neighboring nonbonded interactions.[6] In ref. 6 we also give simple rules to deduce the matrix elements between Rumer structures. It is obvious from eqn. (8) that the energy of ethylene is lowered relative to the spin-alternate determinant by λ.

Parameterization of λ

For polyenes, λ was originally determined using ethylene[4] and subsequently extracted from butadiene[6] which is a somewhat more typical "polyene" (for a similar approach see ref. 18). The spin-free VB method shows that the ground state energy of butadiene with uniform C–C bond lengths is lowered relative to the spin-alternant determinant by $\sqrt{3}\lambda$. Therefore, the ground state value of λ may be determined as follows:

$$\lambda_{\rm CC} = \frac{\sqrt{3}}{3} [E_{\rm sa} - E(1\,{}^1{\rm A_g})], \tag{9}$$

where $E(1\,{}^1{\rm A_g})$ is the energy of the $1\,{}^1{\rm A_g}$ ground state obtained from DFT calculations.[6] By changing the uniform bond length r of butadiene, one has $\lambda_{\rm CC}$ as a function of the bond length,

$$\lambda_{\rm CC} = 0.6850 - 0.6722 r_{\rm CC} + 0.1720 r_{\rm CC}^2 \tag{10}$$

where $\lambda_{\rm CC}$ is in $E_{\rm h}$ and $r_{\rm CC}$ in Å.

From $\lambda_{\rm CC}$ for the C–C bond, one can determine $\lambda_{\rm CO}$ for the C=O bond in 2-propenal. Scheme 2 shows Rumer structures of 2-propenal. The same method applies to the $\lambda_{\rm CN}$ parameter. Thus using $\lambda_{\rm CX}$ (X = O, N), we can rely on eqn. (6) to derive the energies of the two Rumer structures as follows:

$$E_1 = E_{\rm sa} - \lambda_{\rm CC}(1) + \frac{1}{2}\lambda_{\rm CC}(2) - \lambda_{\rm CX}(3) \quad {\rm X = O,\ N} \tag{11}$$

$$E_2 = E_{\rm sa} + \frac{1}{2}\lambda_{\rm CC}(1) - \lambda_{\rm CC}(2) + \frac{1}{2}\lambda_{\rm CX}(3) \quad {\rm X = O,\ N} \tag{12}$$

Similarly, their interaction matrix element[6] and overlap become:

$$H_{12} = -\frac{1}{2}E_{\rm sa} + \frac{1}{2}\lambda_{\rm CC}(1) - \lambda_{\rm CC}(2) + \frac{1}{2}\lambda_{\rm CN}(3) \tag{13}$$

$$S_{12} = -\frac{1}{2} \tag{14}$$

By solving the secular equation of the two Rumer functions, one can express the total energy E in terms of $E_{\rm sa}$ and the parameters $\lambda_{\rm CC}$ and $\lambda_{\rm CX}$. Obviously, given E, $E_{\rm sa}$, and $\lambda_{\rm CC}$, one can determine $\lambda_{\rm CX}$. In the present paper, both E and $E_{\rm sa}$ are taken from the DFT calculations, as explained before.[6]

By changing the bond length $r_{\rm CO}$ in C_3H_4O and $r_{\rm CN}$ in C_3H_5N and optimizing all other geometric parameters of the two molecules, one finds λ as a function of bond length as follows:

$$\lambda_{\rm CO} = 0.9415 - 1.0418 r_{\rm CO} + 0.3031 r_{\rm CO}^2 \tag{15}$$

$$\lambda_{\rm CN} = 0.9038 - 0.9920 r_{\rm CN} - 0.2869 r_{\rm CN}^2 \tag{16}$$

Before proceeding, it is important to note that the use of long bond structures, such as Rumer 2 in Scheme 2, is equivalent to the inclusion of configuration interaction in a molecular orbital treatment.[1,4,6] In fact, in butadiene and glyoxal, *etc.*, the doubly excited molecular orbital configuration corresponds to a long bond structure. As such, the VB wavefunction in VBDFT(s) accounts for the static Coulomb correlation of the electrons, whereas the scaling of λ ensures the incorporation of some dynamic correlation effects on the energy.

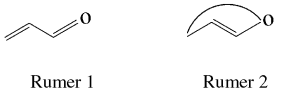

Scheme 2 Rumer structures of C_3H_5O.

The Rumer basis and its truncation

All the Rumer structures of a given chemical structure form an irreducible representation basis set of symmetric group S_M. Thus, the total number of Rumer structures is the dimension (d) of the irrep. $[\mu]=[2^{M/2-S}, 1^{2S}]$.

$$d_{\text{full}} = \binom{M}{M/2-S} - \binom{M}{M/2-S-1} \tag{17}$$

By diagonalizing the basis set, one can obtain a spectrum of the covalent states. For even-membered systems the structure with the lowest energy is the fundamental Rumer structure, which involves $M/2$ short bonds, while for odd-membered systems the fundamental Rumer structure is a set of $(M+1)/2$ Rumer structures which involve $(M-1)/2$ short bonds and an unpaired electron. Scheme 3 shows the spectra of Rumer structures for C_5H_6O and C_4H_5O. It can be seen that the energy spectrum of C_5H_6O is grouped into three blocks; the first block includes the fundamental Rumer structure, the second covers all Rumer structures with two short bonds, and the last is the Rumer structure with a single short bond. For C_4H_5O, the first block includes three quasi-degenerate Rumer structures with two short bonds, of which the Rumer structure where the unpaired electron is at the middle site is the lowest in energy. The second block involves the Rumer structures with only one short bond. This is the general hierarchy of the Rumer structures. Above the first block that includes all the fundamental structures, with the maximum number of short bonds, there lie blocks with fewer and fewer short bonds; the highest having only one short bond. These blocks are then ordered relative to the fundamental block according to their excitation rank; the block with one fewer short bond is singly excited, with two fewer is doubly excited, and so on.[6]

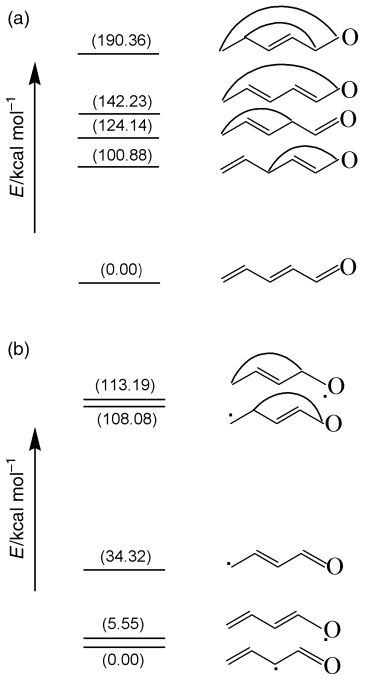

Scheme 3 (a) Energy spectrum of the Rumer structures for C_5H_6O. (b) Energy spectrum of the Rumer structures for C_4H_5O.

If one focuses on the ground states of the systems, it is clear that the higher the energy of a given structure the less important it is to the ground state. To save computational time, truncation of Rumer structures is required for the larger systems. The truncation is classified by hierarchy of excitations. Thus, VB(S), VB(S,D) and VB(S,D,T) correspond, respectively, to inclusion of only singly, singly plus doubly, and singly, doubly, and triply excited Rumer structures in addition to the fundamental one(s). For $M=2n$ (even), the number of Rumer structures at each excitation block are given as follows:

$$d_1 = \binom{n}{2}, \tag{18}$$

$$d_2 = 2\binom{n}{4} + \binom{n}{3}, \tag{19}$$

$$d_3 = 5\binom{n}{6} + 5\binom{n}{5} + \binom{n}{4}, \tag{20}$$

For $M=2n-1$, one can have

$$d_1 = 2\binom{n}{3}, \tag{21}$$

$$d_2 = 5\binom{n}{5} + 2\binom{n}{4}, \tag{22}$$

$$d_3 = 14\binom{n}{7} + 12\binom{n}{6} + 2\binom{n}{5} \tag{23}$$

It can be seen from the above equations that the number of structures for odd-membered systems is much greater than that for even-membered systems at the same level of excitation.

A truncation technique was used in our previous paper,[6] which showed that for even-membered systems VB(S,D,T) gives excellent results for both the ground state and the first excited state, while VB(S,D) is very good for the calculation of the ground state alone. In the present paper we also adopt the truncation technique for larger systems.

All geometries of the systems in the paper are optimized at the level of B3LYP/D95V using GAUSSIAN 98.[21] VBDFT(s) is applied to the series of linear polyenes with heteroatoms, shown in Scheme 1, $C_{M-1}H_MO$, $C_{M-2}H_{M-2}O_2$, $C_{M-1}H_MN$ and $C_{M-2}H_{M-2}N_2$, ($M=4$–26). A full Rumer set calculation is applied for $M=4$–18, VB(S,D,T) for $M=19$, 20, and 22, and VB(S,D) for $M=21$, 23–26.

3 Results and discussion

Fig. 1 shows the correlation of the VBDFT(s) energies plotted against the B3LYP energies for $C_{M-1}H_MO$. The correlation shows that the VBDFT(s) and B3LYP total energies are virtually identical. Similar correlations were found for all other systems, but their plots are not shown for the sake of brevity. The energy differences between VBDFT(s) and B3LYP are shown in Tables 1 and 2. It can be seen from Table 1 that for the even-numbered systems, the VBDFT(s) energies are in good agreement with B3LYP energies. The small systems ($M=4,6$) with two terminal oxygens have the largest deviation, while for $M>6$ the deviation is rather small. Thus, it appears that for these small systems the λ_{CO} parameter underestimates the role of bond polarity, but as the polyene grows this becomes less important.

Table 2 shows the energy differences for M odd. It is seen that the VBDFT(s) energy for the odd-membered systems are lower than those of B3LYP by approximately a constant amount. This shift is due to the fact that λ is determined from even-numbered systems, C_3H_4O and C_3H_5N. Nevertheless, the

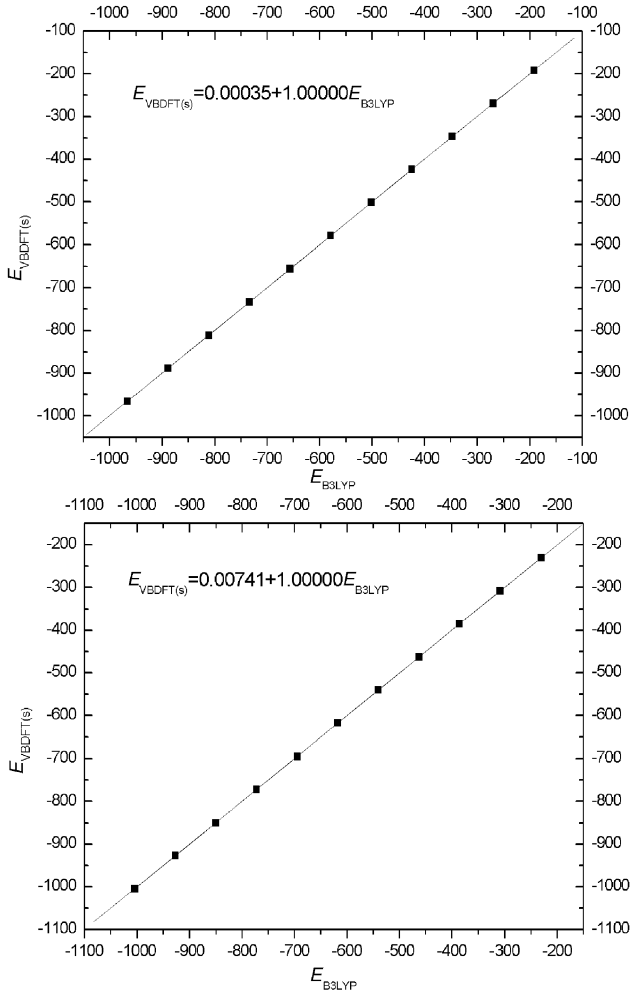

Fig. 1 A plot of the VBDFT(s) energy *vs.* the B3LYP energy for $C_{M-1}H_MO$ species. (a) M even; (b) M odd.

quality of the fit is good. We may therefore conclude that despite the C=X bond polarity in these systems, the set of formally covalent Rumer structures gives a reasonably good representation for heteroatom-substituted polyenes, presumably because ionicity effects are embedded in λ.[4,6]

Table 3 shows the energies of the spin-alternant determinants, which define the energy of the σ-frames with nonbonded p_π electrons (see drawing 1). Also shown are the π bond energies and their increments for the even-numbered series of $C_{M-1}H_MO$, where the π bond energy is defined as the energy difference between the VBDFT(s) energy and that of the spin-alternant determinant. It can be seen that both the VBDFT(s) energies and E_{sa} vary linearly with M. This means that both the σ frame and π bonding share energy additivity with increments of $77.332 + 0.001\ E_h$ for the σ frame, and of 77.396 E_h for the total energies. The difference between these increments is the π increment for a C–C unit of *ca.* 40 kcal mol^{-1}.[22] All other series possess these properties too, but for the sake of brevity we do not present here the details. This additivity of π and σ energies in linear polyenes is well known.[23,24] The fact that VBDFT(s) reproduces this additivity is a good indication both for the validity of the method, as well as for the correctness of the additivity that emerges from a variety of methods.[14,23,24]

Insight into the nature of the ground state can be obtained by looking at a VB mixing diagram of the Rumer structures. Two simple examples are shown for even- and odd-membered systems in Schemes 4 and 5, respectively. Scheme 4 shows the mixing diagram for the smallest even-membered polyene that possesses two Rumer structures.[6] Irrespective of the nature of the group X, the fundamental Rumer structure (R_1) is lower than the singly excited one (R_2). Consequently, the ground state (Ψ_0) will be primarily R_1, with a smaller contribution of R_2. The energy gap between the Rumer structures is larger for heteroatoms, but so is the matrix element that varies in proportion to λ.[6] Consequently, the substituted even-membered polyenes are rather similar to their all-carbon parents. Scheme 5 shows the situation for the smallest odd member.[25,26] Here the all-carbon system has two degenerate Rumer structures and the ground state will have equal contributions from both. In contrast, in the heteroatom-substituted system, the Rumer with the double bond across C=X is lower in energy since λ for this bond is larger than for the C=C. Consequently, the ground state will now resemble the more stable Rumer structure and the spin distribution will reside mainly on the terminal carbon and to a smaller extent on the heteroatom X. As the polyene grows, there will be more Rumer structures. In the even-membered family the ground state will contain more and more contributions from excited Rumer structures that will mix to an extent inversely proportional to the rank of excitation. In the odd-membered system, the number of the Rumer structures that are quasi-degenerate with the fundamental structure will grow too, and this in addition to the mixing of the more highly excited Rumer structures will create a highly mixed ground state.

These mixing patterns can be traced systematically with the VBDFT(s) method should one wish. For brevity, Fig. 2 shows the weights of the fundamental structures against the number of π bonds. For the even-numbered systems (Fig. 2a), the fundamental Rumer structure possesses the highest weight in the wavefunction, which decreases with the chain lengths (*e.g.* in C_3H_5O $w_0 = 0.88$, while in $C_{26}H_{25}O$ $w_0 = 0.08$). For the

Table 1 Energy differences (kcal mol^{-1}) between VBDFT(s) and B3LYP for the even-membered systems

M	$\Delta E(C_{M-1}H_MO)^a$	$\Delta E(C_{M-2}H_{M-2}O_2)$	$\Delta E(C_{M-1}H_{M+1}N)$	$\Delta E(C_{M-2}H_MN_2)$
4	0.01	11.92	0.58	4.29
6	0.09	5.78	1.01	2.45
8	−0.21	2.70	1.10	2.09
10	0.35	1.80	2.21	2.97
12	0.12	0.67	1.93	2.65
14	0.72	0.59	2.68	2.77
16	0.53	0.01	2.60	2.55
18	1.04	0.11	3.27	3.04
20	0.93	−0.24	3.19	2.95
22	1.53	−0.04	3.77	3.42
24	0.23	−1.95	1.83	1.49
26	−0.82	−2.59	1.49	1.06
Mean error	0.38 ± 0.48	1.56 ± 2.53	2.14 ± 0.73	2.64 ± 0.61

[a] $\Delta E = E_{VBDFT(s)} - E_{B3LYP}$.

Table 2 Energy differences (kcal mol^{-1}) between VBDFT(s) and B3LYP for the odd-membered systems

M	$\Delta E(C_{M-1}H_MO)^a$	$\Delta E(C_{M-2}H_{M-2}O_2)$	$\Delta E(C_{M-1}H_{M+1}N)$	$\Delta E(C_{M-2}H_MN_2)$
5	− 4.56	3.78	− 3.21	− 2.01
7	− 5.47	− 1.81	− 0.49	− 2.91
9	− 4.69	− 2.94	− 3.32	− 2.77
11	− 5.50	− 4.87	− 3.93	− 3.71
13	− 5.88	− 4.93	− 3.15	− 3.11
15	− 5.47	− 6.22	− 3.76	− 3.96
17	− 4.97	− 5.97	− 2.91	− 3.33
19	− 5.72	− 7.00	− 3.81	− 4.03
21	− 5.27	− 6.81	− 3.26	− 3.70
23	− 6.11	− 7.91	− 4.11	− 3.63
25	− 5.90	− 7.84	− 3.80	− 4.27
Mean error	− 5.41 ± 0.43	− 4.77 ± 2.41	− 3.25 ± 0.66	− 3.22 ± 0.50

[a] $\Delta E = E_{VBDFT(s)} - E_{B3LYP}$.

Table 3 Energy analysis for the even-membered $C_{M-1}H_MO$ species

M	E^a_{sa}/E_h	E^b_π/E_h	ΔE^c_π/kcal mol^{-1}	$\Delta E^d_{VBDFT(s)}/E_h$	$\Delta E^e_{sa}/E_h$
4	− 191.70496	− 0.17992			
6	− 269.03680	− 0.24397	− 40.19202	− 77.39589	− 77.33184
8	− 346.36816	− 0.30804	− 40.20457	− 77.39543	− 77.33136
10	− 423.70070	− 0.37230	− 40.32379	− 77.39680	− 77.33254
12	− 501.03231	− 0.43629	− 40.15436	− 77.39560	− 77.33161
14	− 578.36532	− 0.50017	− 40.08534	− 77.39689	− 77.33301
16	− 655.69715	− 0.56400	− 40.05396	− 77.39566	− 77.33183
18	− 733.03050	− 0.62738	− 39.77158	− 77.39673	− 77.33335
20	− 810.36205	− 0.69059	− 39.66491	− 77.39746	− 77.33155
22	− 887.69495	− 0.75556	− 40.76932	− 77.39787	− 77.33290
24	− 965.02702	− 0.81660	− 38.30321	− 77.39311	− 77.33207
26	− 1042.3600	− 0.87860	− 38.90562	− 77.39489	− 77.33298

[a] Energies of the spin-alternant determinants (see drawing 1). [b] π energies, defined as $E_\pi = E_{VBDFT(s)} - E_{sa}$. [c] π bond energy increments, defined as $\Delta E_\pi = E_\pi(M) - E_\pi(M-1)$. [d] VBDFT(s) energy increments, defined as $\Delta E_{VBDFT(s)} = E_{VBDFT(s)}(M) - E_{VBDFT(s)}(M-1)$. [e] E_{sa} increments, defined as $\Delta E_{sa} = E_{sa}(M) - E_{sa}(M-1)$.

odd-numbered systems (Fig. 2b), the fundamental weight comes from n quasi-degenerate Rumers with $n-1$ short bonds. Here too, this weight decreases with chain length. It is also seen that the weights for the fundamental Rumer structures for various series are almost identical.

A projection to $M = \infty$ shows that for infinitely long polyenes the weight of the fundamental Rumer will be

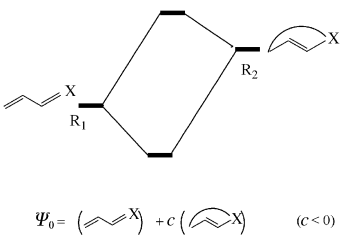

Scheme 4 VB mixing diagram for C_4H_4X (X = CH_2, NH, O).

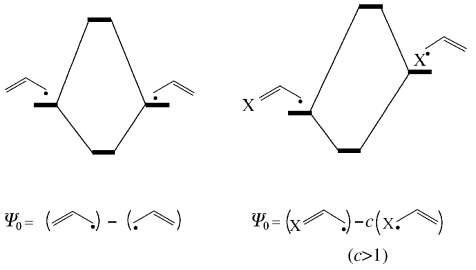

Scheme 5 VB mixing diagram for C_3H_5 and C_2H_3X (X = CH_2, NH, O).

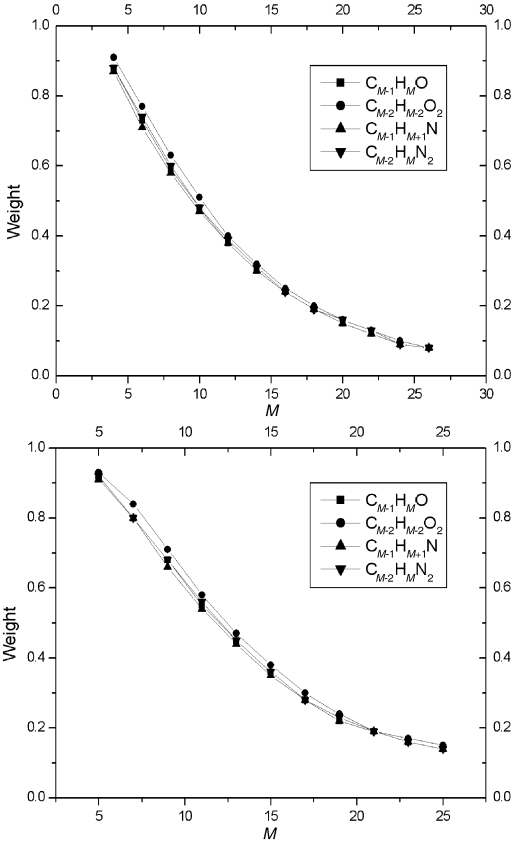

Fig. 2 A plot of the weights of the fundamental structures *vs.* the numbers of heavy atoms. (a) M even; (b) M odd.

Table 4 π-resonance energies for the even-membered systems (kcal mol^{-1})

M	RE ($C_{M-1}H_MO$)[a,b]	RE ($C_{M-2}H_{M-2}O_2$)	RE ($C_{M-1}H_{M+1}N$)	RE ($C_{M-2}H_MN_2$)
4	6.02(3.01)	4.17(2.09)	6.62(3.31)	5.69(2.85)
6	14.63(4.88)	12.34(4.11)	15.20(5.07)	14.04(4.68)
8	24.00(6.00)	21.47(5.37)	24.50(6.13)	23.19(5.80)
10	33.68(6.74)	31.30(6.26)	34.10(6.82)	33.47(6.69)
12	43.60(7.27)	41.18(6.86)	43.93(7.32)	42.68(7.11)
14	53.69(7.67)	51.33(7.33)	53.91(7.70)	52.60(7.51)
16	63.86(7.98)	61.64(7.71)	64.00(8.00)	62.75(7.84)
18	74.32(8.26)	71.88(7.99)	74.14(8.24)	72.83(8.09)
20	84.37(8.44)	82.88(8.29)	84.27(8.43)	83.11(8.31)
22	94.60(8.60)	92.56(8.41)	94.45(8.59)	93.34(8.49)
24	103.02(8.59)	101.31(8.44)	102.81(8.57)	102.01(8.50)
26	112.45(8.65)	110.81(8.52)	112.22(8.63)	111.38(8.57)

[a] $RE = E_{VBDFT(s)}(R_1) - E_{VBDFT(s)}$, where R_1 is the fundamental structure. [b] Values in parentheses are resonance energy per bond.

Table 5 Resonance energies for the odd-membered systems (kcal mol^{-1})

M	RE ($C_{M-1}H_MO$)[a,b]	RE ($C_{M-2}H_{M-2}O_2$)	RE ($C_{M-1}H_{M+1}N$)	RE ($C_{M-2}H_MN_2$)
5	33.69(16.85)	33.07(16.54)	35.48(17.74)	33.53(16.77)
7	48.06(16.02)	44.70(14.90)	47.87(15.96)	48.98(16.33)
9	60.93(15.26)	56.75(14.19)	62.05(15.51)	60.98(15.25)
11	73.59(14.72)	70.72(14.14)	74.90(14.98)	73.49(14.70)
13	85.11(14.35)	82.51(13.75)	86.53(14.42)	84.85(14.14)
15	98.13(14.02)	95.45(13.64)	98.80(14.11)	97.35(13.91)
17	109.73(13.72)	107.01(13.38)	110.30(13.79)	108.74(13.59)
19	122.08(13.56)	119.39(13.27)	122.43(13.60)	121.12(13.46)
21	133.25(13.33)	130.81(13.08)	133.77(13.38)	132.51(13.25)
23	144.97(13.18)	143.05(13.00)	145.56(13.23)	144.28(13.12)
25	156.40(13.03)	154.36(12.86)	156.76(13.06)	155.54(12.96)

[a] $RE = E_{VBDFT(s)}(R_1) - E_{VBDFT(s)}$, where R_1 is the fundamental structure. [b] Values in parentheses are resonance energy per bond.

smaller than 0.01. The same observation was made for the C_MH_{M+2} series.[6] This means that long polyenes are a far cry from the usual localized structure used in textbooks to describe them. They are in fact highly delocalized species that contain an extensive mixture from all the excited Rumer structures. Considering the fact that the Rumer structures involve spin-pairing of the p_π electrons across long bonds, these electrons are in fact diradical pairs or solitons. One might therefore say that long polyenes with or without heteroatoms are best represented by a collection of delocalized solitons. Why is the π-energy additive while the electronic structure is so delocalized? An answer is provided by the π-resonance energies, which are defined as the difference between the total π-energy and the π-energy of the fundamental Rumer structure.

Tables 4 and 5 show the π-resonance energies for all the series. It can be seen that the resonance energies per bond are almost constant for the two series. Clearly, the resonance energy is also additive. Therefore, despite the extensively delocalized nature of the polyenes their total energy exhibits additivity. Inspection of the values shows that for the systems with one heteroatom the resonance energies are a little higher than those of the systems with two heteroatoms. This makes physical sense. Furthermore, the values for the odd-membered systems are higher than those for even-membered systems, which again makes sense, since the odd-membered systems have a set of quasi-degenerate Rumer structures.

4 Conclusion

The results show that the VBDFT(s) can be adapted to systems containing heteroatoms (X), and that bond polarity effects are largely contained in the effective parameter used to model the C=X bond. The method provides clear insight into the nature of small and large polyenes in terms of VB mixing of Rumer structures that are the familiar chemical structures. The resulting insight resembles in its lucidity the corresponding insight that emerges from orbital interaction used in molecular orbital theory.[3] The next major goal is to apply the method to cyclic systems, and to systems which exhibit state degeneracies (*e.g.* trimethylene methane, *etc.*). Achievement of this goal will provide tools to obtain insight into electronic structure of species related to nanotubes in terms of their chemical structure.

Acknowledgements

The research at XMU is supported by the Natural Science Foundation of China (No. 20073033, No. 29892166, and No. 20023001). The research at HU is supported by the VW Stiftung through the Ministry of Sciences of the Niedersachsen States.

References

1 P. C. Hiberty, *J. Mol. Struct.* (*THEOCHEM*) 1998, **451**, 237.
2 S. Shaik and A. Shurki, *Angew. Chem., Int. Ed. Engl.*, 1999, **38**, 586.
3 R. Hoffmann, *J. Mol. Struct.* (*THEOCHEM*), 1988, **424**, 1.
4 W. Wu, S. Zhong and S. Shaik, *Chem. Phys. Lett.*, 1998, **292**, 7.
5 R. Pauncz, *Spin Eigenfunctions. Construction and Use*, Plenum, New York, 1979.
6 W. Wu, D. Danovich, A. Shurki and S. Shaik, *J. Phys. Chem. A*, 2000, **104**, 8744.
7 L. Serrono-Andrés, M. Merchán, I. Nebot-Gil, R. Lindh and B. O. Roos, *J. Chem. Phys.*, 1993, **98**, 3151.
8 L. Serrono-Andrés, I. Nebot-Gil, R. Lindh, B. O. Roos and M. Merchán, *J. Phys. Chem.*, 1993, **97**, 9360.

9 In SCVB and GVB theories, ionicity is embedded in the distortion of the atomic orbitals (see refs. 10 and 11). See, however, explicit treatment of ionicity in ref. 12.
10 D. L. Cooper, J. Gerratt and M. Raimondi, *Adv. Chem. Phys.*, 1987, **69**, 319.
11 W. A. Goddard, III and B. L. Harding, *Annu. Rev. Phys. Chem.*, 1978, **29**, 363.
12 P. C. Hiberty, S. Humbel, C. P. Byrman and J. H. van Lenthe, *J. Chem. Phys.*, 1994, **101**, 5969.
13 J. P. Malrieu and D. Maynau, *J. Am. Chem. Soc.*, 1982, **104**, 3021.
14 M. Said, D. Maynau, J. P. Malrieu and M. A. G. Bach, *J. Am. Chem. Soc.*, 1984, **106**, 571.
15 M. Said, D. Maynau and J. P. Malrieu, *J. Am. Chem. Soc.*, 1984, **106**, 580.
16 J. P. Malrieu, in *Theoretical Models of Chemical Bonding*, ed. Z. B. Maksic, Springer, Berlin, 1990, p. 107.
17 D. J. Klein, H. Zhu, R. Valenti and M. A. Garcia-Bach, *Int. J. Quantum Chem.*, 1997, **65**, 421.
18 J. Wu and D. L. Cooper, *Phys. Chem. Chem. Phys.*, 2001, **3**, 2419.
19 R. McWeeny, *Int. J. Quantum Chem.*, 1988, **34**, 25.
20 W. Wu, Y. Mo and Q. Zhang, *J. Mol. Struct.* (*THEOCHEM*), 1993, **283**, 227.
21 GAUSSIAN 98, M. J. Frisch, G. W. Trucks, H. B. Schlegel, G. E. Scuseria, M. A. Robb, J. R. Cheeseman, V. G. Zakrzewski, J. A. Montgomery, Jr., R. E. Stratmann, J. C. Burant, S. Dapprich, J. M. Millam, A. D. Daniels, K. N. Kudin, M. C. Strain, O. Farkas, J. Tomasi, V. Barone, M. Cossi, R. Cammi, B. Mennucci, C. Pomelli, C. Adamo, S. Clifford, J. Ochterski, G. A. Petersson, P. Y. Ayala, Q. Cui, K. Morokuma, D. K. Malick, A. D. Rabuck, K. Raghavachari, J. B. Foresman, J. Cioslowski, J. V. Ortiz, A. G. Baboul, B. B. Stefanov, G. Liu, A. Liashenko, P. Piskorz, I. Komaromi, R. Gomperts, R. L. Martin, D. J. Fox, T. Keith, M. A. Al-Laham, C. Y. Peng, A. Nanayakkara, M. Challacombe, P. M. W. Gill, B. Johnson, W. Chen, M. W. Wong, J. L. Andres, C. Gonzalez, M. Head-Gordon, E. Replogle, and J. A. Pople, Gaussian, Inc., Pittsburgh, PA, 1998.
22 The increment involves the π-bond energy ($-\lambda$) and the non-bonded repulsion.
23 M. J. S. Dewar and C. de Llano, *J. Am. Chem. Soc.*, 1969, **91**, 789.
24 B. A. Hess, Jr, and L. J. Schaad, *J. Am. Chem. Soc.*, 1983, **105**, 7500.
25 P. B. Karadakov, J. Gerratt, G. Raos, D. L. Cooper and M. Raimondi, *J. Am. Chem. Soc.*, 1994, **116**, 2075.
26 Y. Mo, Z. Lin, W. Wu and Q. Zhang, *J. Phys. Chem.*, 1996, **100**, 11 569.